

Assessment of Temperature Induced Fracture in Boron Nitride/AA1100 Alloy Particle-Reinforced Metal Matrix Composites

¹S. Sundara Rajan and A. Chennakesava Reddy²

¹Scientist -G, Defence Research and Development Organisation, Hyderabad, India.

²Associate Professor, Department of Mechanical Engineering, Vasavi College of Engineering, Hyderabad, India
dr_acreddy@yahoo.com

Abstract: *In the present work, the AA1100/BN metal matrix composites were fabricated at 10% and 30% volume fractions of BN. The composites were subjected to structural and thermal loads. The microstructure of AA1000 alloy/BN reveals the occurrence of interphase debonding and matrix damage. The FEA results confirm the experimental results.*

Keywords: *AA1100, boron nitride, spherical nanoparticle, RVE model, finite element analysis, debonding, matrix damage.*

1. INTRODUCTION

Interphase, or interface in particle-reinforced composite materials are the thin layers between the particle and matrix as shown in figure 1. The interphase is formed due to chemical reactions between the particle and matrix materials. Different levels of stresses and deformations can develop in the particle and matrix materials, because of this mismatch in the material properties. Although small in thickness, interphases can significantly affect the overall mechanical properties of the particle-reinforced composites, as observed in many studies [1, 2]. It is the weakest link in the load path, and consequently most failures in particle reinforced composites, such as debonding and matrix cracking, occur in or near this region. Thus, it is crucial to fully understand the mechanism and effects of the interphases in fiber-reinforced composites. Many finite element models based on the two-dimensional elasticity theory have been developed to study the micromechanical properties of particle-reinforced composites [3-18].

Boron nitride (BN) has been well studied for applications including ceramic and polymer nanocomposites. Nanoscale boron nitride is essential for applications as the increased surface area resulting in better incorporation in the matrix. BN possesses a number of material properties which increase its utility in machining and coating applications including wear resistance; chemical and thermal stability and wide band gap. In this paper, the effect of temperature on the fracture in AA1100 alloy/BN composites was investigated. The shape BN nanoparticle considered in this work is spherical. The periodic particle distribution was a square array as shown in figure 1.

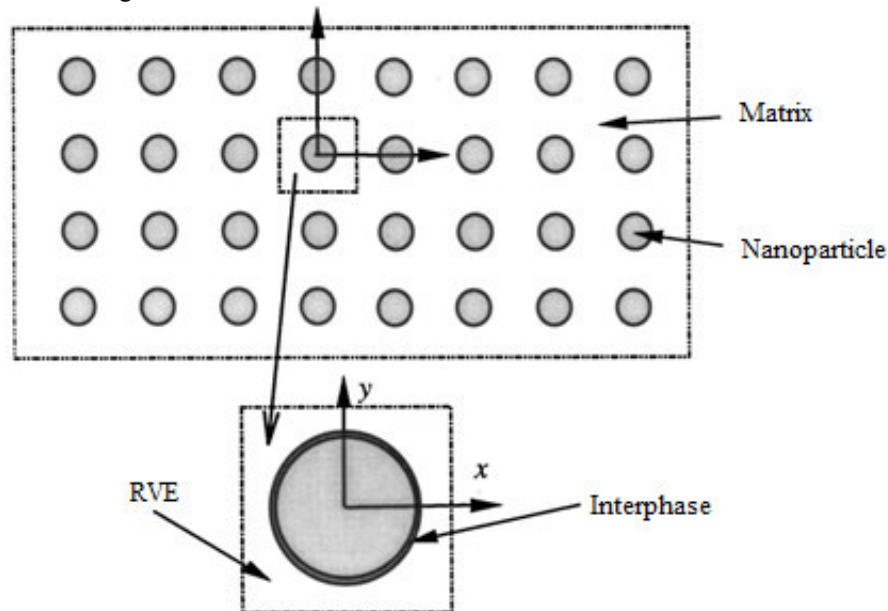


Figure 1: The interphase in a nanoparticle-reinforced composite.

2. MATERIALS METHODS

The matrix material was AA1100 alloy. The reinforcement material was BN nanoparticles of average size 100nm. The mechanical properties of materials used in the present work are given in table 1.

Table 1: Mechanical properties of AA1100 matrix and BN nanoparticles

Property	AA1100	BN
Density, g/cc	2.71	6.15
Elastic modulus, GPa	68.9	400
Coefficient of thermal expansion, $10^{-6} 1/^{\circ}\text{C}$	21.8	5.5
Specific heat capacity, $\text{J/kg}^{\circ}\text{C}$	904	1150
Thermal conductivity, $\text{W/m}^{\circ}\text{C}$	220	52
Poisson's ratio	0.33	0.19

AA1100 alloy/BN composites were fabricated by the stir casting process and low pressure casting technique with argon gas at 3.0 bar. The composite samples were give solution treatment and cold rolled to the predefined size of tensile specimens. The heat-treated samples were machined to get flat-rectangular specimens (figure 2) for the tensile tests. The tensile specimens were placed in the grips of a Universal Test Machine (UTM) with temperature controlled chamber at a specified grip separation and pulled until failure. The test speed was 2 mm/min. A strain gauge was used to determine elongation. In the current work, a cubical representative volume element (RVE) was implemented to analyze the tensile behavior AA1100/BN nanoparticle composites at two (10% and 30%) volume fractions of BN and at different temperatures. The large strain PLANE183 element was used in the matrix in all the models. In order to model the adhesion between the matrix and the particle, a CONTACT 172 element was used.

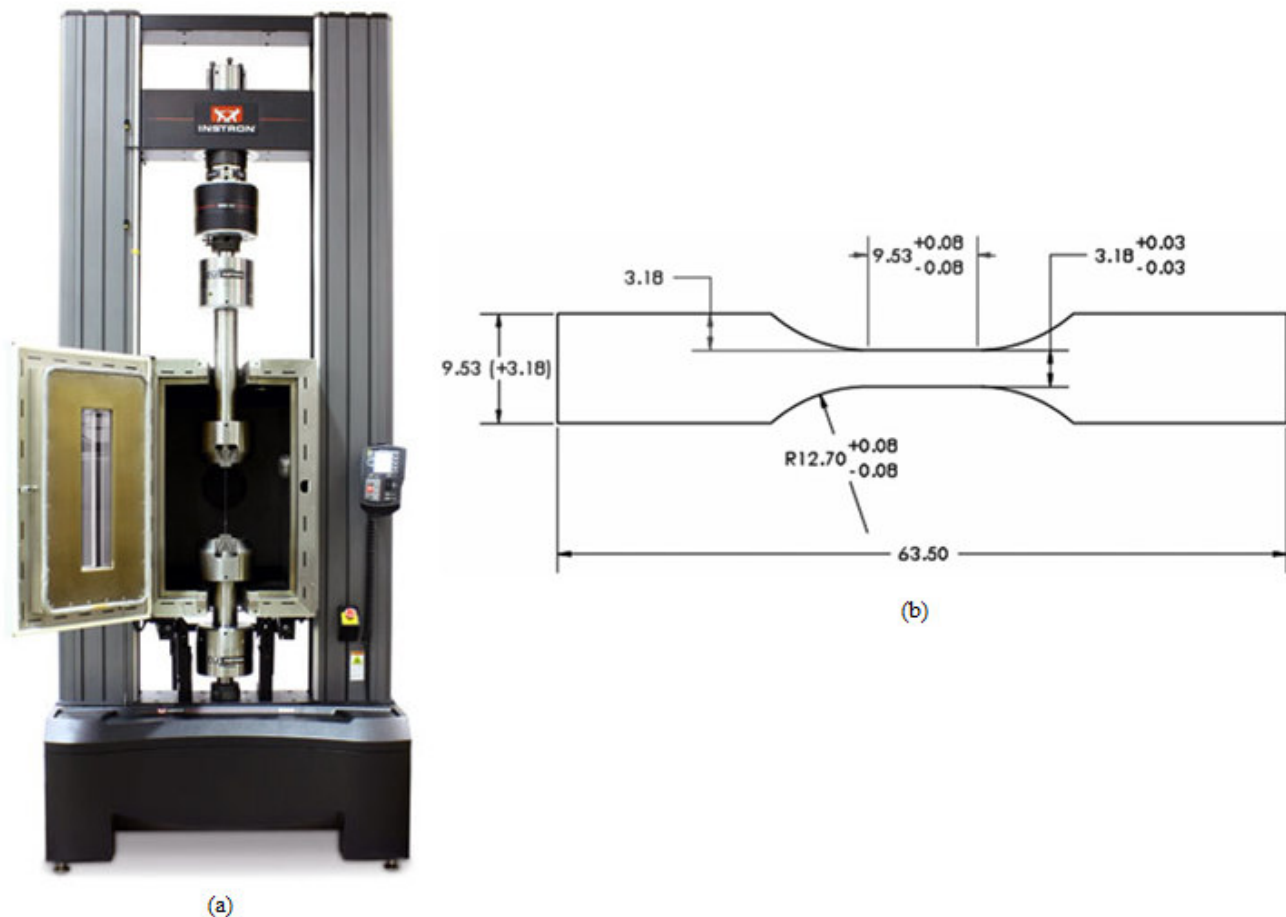


Figure 2: Tensile testing: UTM with temperature controlled chamber and (b) shape and dimensions of tensile specimen.

3. RESULTS AND DISCUSSION

The optical micrograph as shown in figure 3 reveals random distribution of BN (30% Vp) particles in AA1100 alloy matrix.

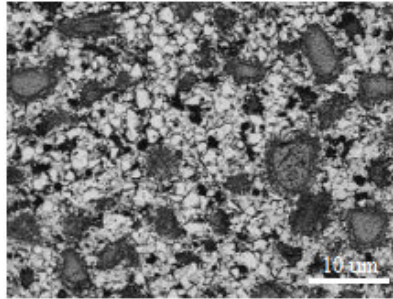


Figure 3: Microstructure showing distribution of 30% BN nanoparticles in AA1100 alloy matrix.

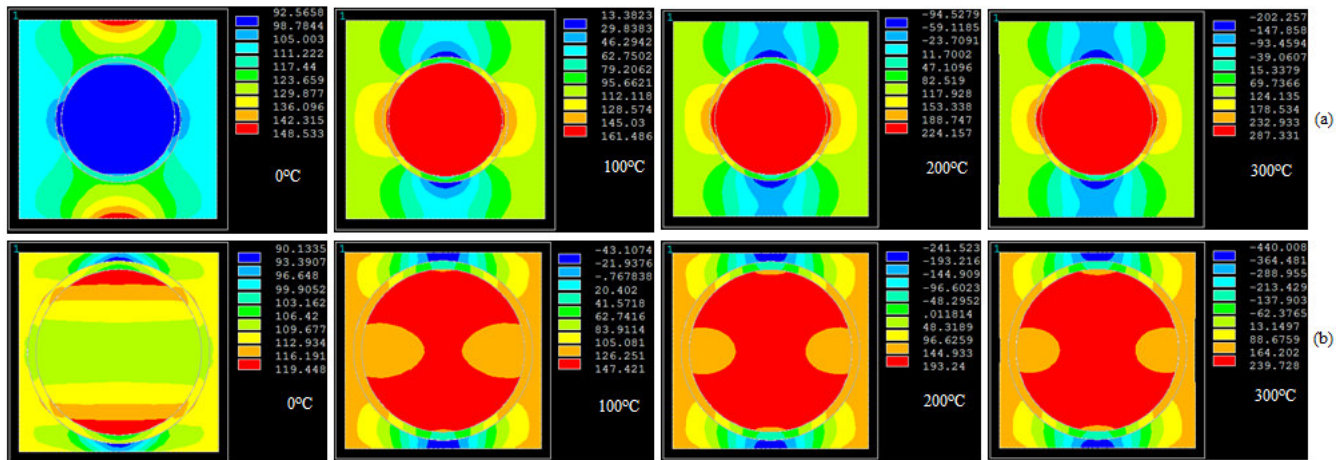


Figure 4: FEA results of tensile stress induced along load direction in the composites comprising of: (a) 10% BN and (b) 30% BN.

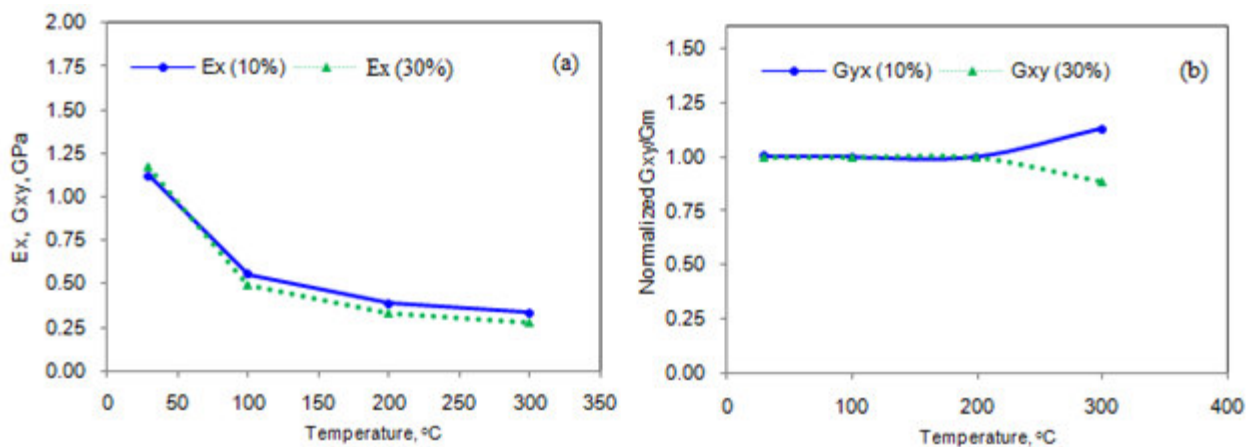


Figure 5: Effect of temperature on stiffness of AA1100/BN composites.

3.1 Micromechanical Behavior

Figure 4 represents the tensile stresses induced in the composites along the load direction. The tensile stress increases with increase of temperature and it decreases with increase of volume fraction of BN in AA1100 alloy matrix. The softening of the composite increases with increase of temperature and accordingly, the range of plastic deformation is extended before the occurrence of final fracture of the composites. The normalized elastic modulus is shown in figure 5a. The elastic modulus is normalized with the elastic modulus of AA1100 alloy. The stiffness of the composites decreases with increase of temperature.

The stiffness of AA1100 alloy/10% BN composites is higher than that of AA1100 alloy/30% BN composites with respect to increase of temperature. Up to temperature of 200°C, the normalized shear modulus is constant with respect to volume fraction of BN. Above 200°C, the shear modulus of AA1100 alloy/10% BN composites increases while it decreases for AA1100 alloy/30% BN composites (figure 5b).

3.2 Fracture Analysis

If the particle deforms in an elastic manner (according to Hooke's law) then,

$$\tau = \frac{n}{2} \sigma_p \quad (1)$$

where σ_p is the particle stress. If particle fracture occurs when the stress in the particle reaches its ultimate tensile strength, $\sigma_{p,uts}$, then setting the boundary condition at

$$\sigma_p = \sigma_{p, uts} \quad (2)$$

The relationship between the strength of the particle and the interfacial shear stress is such that if

$$\sigma_{p, uts} < \frac{2\tau}{n} \quad (3)$$

Then the particle will fracture. From the figure 6b, it is observed that the BN nanoparticle was not fractured as the condition in Eq. (3) is not satisfied. However, the BN nanoparticles in AA1100 alloy/30% BN composites have experienced thermal shocks resulting local stress fields within the particles (figure 7). This is due to CTE mismatch between BN nanoparticles and AA1100 alloy matrix. For the interfacial debonding/yielding to occur, the interfacial shear stress reaches its shear strength:

$$\tau = \tau_{max} \quad (4)$$

For particle/matrix interfacial debonding can occur if the following condition is satisfied:

$$\tau_{max} < \frac{n\sigma_p}{2} \quad (5)$$

It is observed from figure 6a that the interfacial debonding (figure 7) occurs between BN nanoparticle and AA1100 alloy matrix as the condition in Eq.(5) is satisfied.

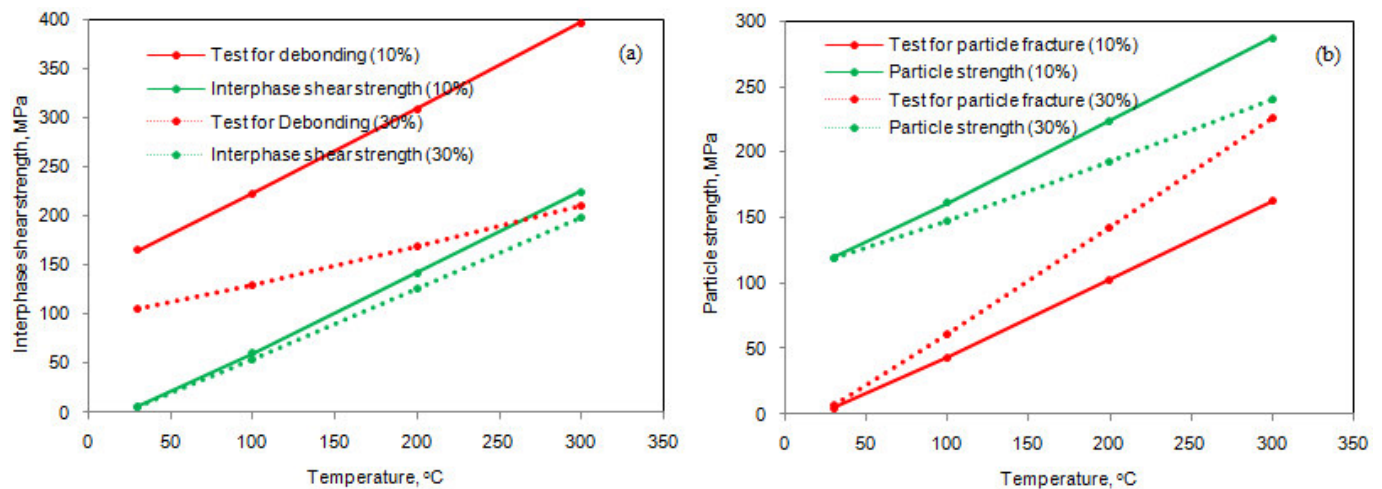


Figure 6: Criterion for interfacial debonding (a) and for particle fracture (b).

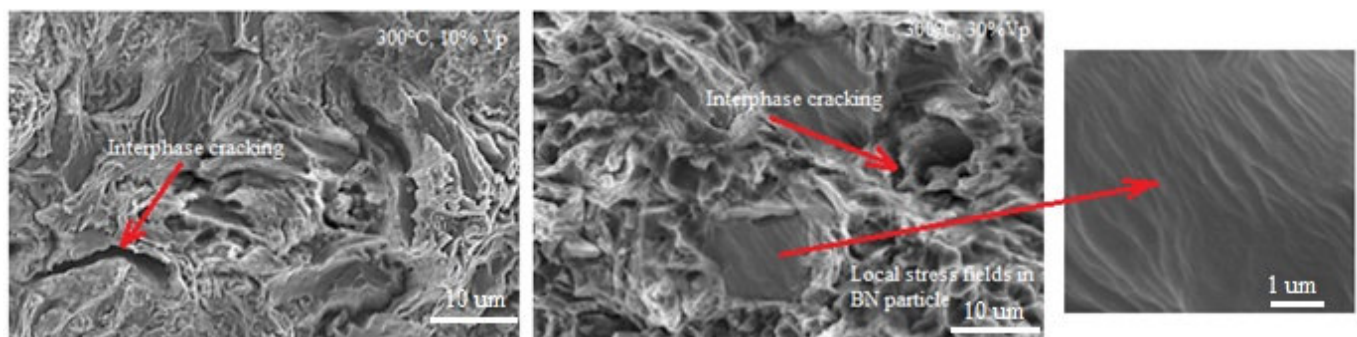


Figure 7: SEM images showing debonding in AA1100/BN composites.

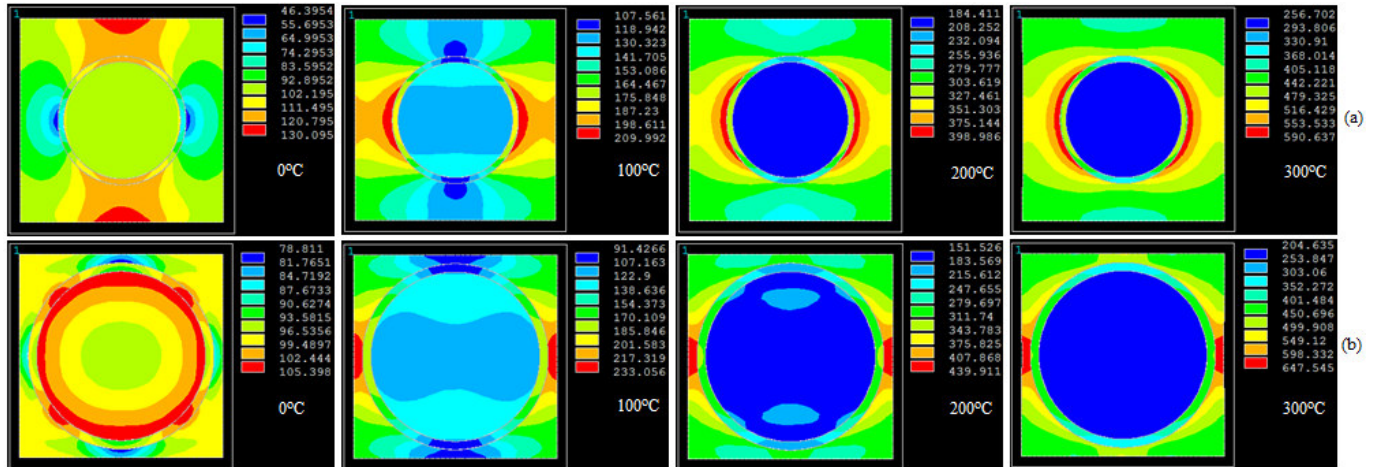


Figure 8: Images of von Mises stresses obtained from FEA: (a) AA1100/10%BN and (b) AA1100/30%BN composites.

As seen from figure 8 the von Mises stress induced at the interface are higher than that induced in the nanoparticle. Hence, the interfacial debonding was occurred between the particle and the matrix. The microstructures (figure 7) confirm the FEA results shown in figure 8. The matrix fracture is also observed in AA1100/ BN composites due to heavy transfer of load from the matrix to the nanoparticle. The interfacial debonding increases with increase of temperature.

4. CONCLUSION

The microstructure of AA1100 alloy/BN composites reveals the presence of interfacial debonding and matrix damage. The results obtained from FEA match with those of experimental procedure. The shear stress is high at the interface leading to interfacial debonding in AA1100/ BN composites due to thermal loading.

REFERENCES

1. K. K. Chawla, Composite Materials: Science and Engineering, Springer-Verlag, New York, 1987.
2. J. D. Achenbach, H. Zhu, Effect of Interphases on Micro and Macromechanical Behavior of Hexagonal-Array Fiber Composites, ASME Journal of Applied Mechanics, 57, 1990, pp. 956–963.
3. A. Chennakesava Reddy, Effect of Particle Loading on Microelastic Behavior and interfacial Traction of Boron Carbide/AA4015 Alloy Metal Matrix Composites, 1st International Conference on Composite Materials and Characterization, Bangalore, March 1997, pp. 176-179.
4. A. Chennakesava Reddy, Reckoning of Micro-stresses and interfacial Traction in Titanium Boride/AA2024 Alloy Metal Matrix Composites, 1st International Conference on Composite Materials and Characterization, Bangalore, March 1997, pp. 195-197.
5. A. Chennakesava Reddy, Evaluation of Debonding and Dislocation Occurrences in Rhombus Silicon Nitride Particulate/AA4015 Alloy Metal Matrix Composites, 1st National Conference on Modern Materials and Manufacturing, Pune, India, 19-20 December 1997, pp. 278-282.
6. A. Chennakesava Reddy, Interfacial Debonding Analysis in Terms of Interfacial Traction for Titanium Boride/AA3003 Alloy Metal Matrix Composites, 1st National Conference on Modern Materials and Manufacturing, Pune, 19-20 December, 1997.
7. A. Chennakesava Reddy, Assessment of Debonding and Particulate Fracture Occurrences in Circular Silicon Nitride Particulate/AA5050 Alloy Metal Matrix Composites, National Conference on Materials and Manufacturing Processes, Hyderabad, India, 27-28 February 1998, pp. 104-109.
8. A. Chennakesava Reddy, Local Stress Differential for Particulate Fracture in AA2024/Titanium Carbide Nanoparticulate Metal Matrix Composites, National Conference on Materials and Manufacturing Processes, Hyderabad, India, 27-28 February 1998, pp. 127-131.
9. A. Chennakesava Reddy, Micromechanical Modelling of Interfacial Debonding in AA1100/Graphite Nanoparticulate Reinforced Metal Matrix Composites, 2nd International Conference on Composite Materials and Characterization, Nagpur, India, 9-10 April 1999, pp. 249-253.

10. A. Chennakesava Reddy, Cohesive Zone Finite Element Analysis to Envisage Interface Debonding in AA7020/Titanium Oxide Nanoparticulate Metal Matrix Composites, 2nd International Conference on Composite Materials and Characterization, Nagpur, India, 9-10 April 1999, pp. 204-209.
11. B. Kotiveera Chari, A. Chennakesava Reddy, Debonding Microprocess and interfacial strength in ZrC Nanoparticle-Filled AA1100 Alloy Matrix Composites using RVE approach, 2nd National Conference on Materials and Manufacturing Processes, Hyderabad, India, 10-11 March 2000, pp. 104-109.
12. A. Chennakesava Reddy, Micromechanical and fracture behaviors of Ellipsoidal Graphite Reinforced AA2024 Alloy Matrix Composites, 2nd National Conference on Materials and Manufacturing Processes, Hyderabad, India, 10-11 March 2000, pp. 96-103.
13. S. Sundara Rajan, A. Chennakesava Reddy, Micromechanical Modeling of Interfacial Debonding in Silicon Dioxide/AA3003 Alloy Particle-Reinforced Metal Matrix Composites, 2nd National Conference on Materials and Manufacturing Processes, Hyderabad, India, 10-11 March 2000, pp. 110-115.
14. S. Sundara Rajan, A. Chennakesava Reddy, Role of Volume Fraction of Reinforcement on Interfacial Debonding and Matrix Fracture in Titanium Carbide/AA4015 Alloy Particle-Reinforced Metal Matrix Composites, 2nd National Conference on Materials and Manufacturing Processes, Hyderabad, India, 10-11 March 2000, 116-120.
15. A. Chennakesava Reddy, Constitutive Behavior of AA5050/MgO Metal Matrix Composites with Interface Debonding: the Finite Element Method for Uniaxial Tension, 2nd National Conference on Materials and Manufacturing Processes, Hyderabad, India, 10-11 March 2000, pp. 121-127.
16. B. Kotiveera Chari, A. Chennakesava Reddy, Interfacial Debonding of Boron Nitride Nanoparticle Reinforced 6061 Aluminum Alloy Matrix Composites, 2nd National Conference on Materials and Manufacturing Processes, Hyderabad, India, 10-11 March 2000, pp. 128-133.
17. P. M. Jebaraj, A. Chennakesava Reddy, Simulation and Microstructural Characterization of Zirconia/AA7020 Alloy Particle-Reinforced Metal Matrix Composites, 2nd National Conference on Materials and Manufacturing Processes, Hyderabad, India, 10-11 March 2000, pp. 134-140.
18. P. M. Jebaraj, A. Chennakesava Reddy, Continuum Micromechanical modeling for Interfacial Debonding of TiN/AA8090 Alloy Particulate Composites, 2nd National Conference on Materials and Manufacturing Processes, Hyderabad, India, 10-11 March 2000, pp. 141-145.